

The Structure and Mechanical Properties of Bridge Steel Weldings With Glass-Steel Liners

V N Muzalev¹, B S Semukhin^{1,2}, V I Danilov^{2,3}

¹Tomsk State Architecture and Building University
2, Solyanaya sq., Tomsk, 634003, Russia

²Institute of Strength Physics and Materials Science SB RAS
2/4, Akademicheskoy pr., Tomsk, 634055, Russia

³Yurga Institute of Technology National Research Tomsk Polytechnic University
26, Leningradskaya st., Yurga, Kemerovo region, 652055, Russia

E-mail: dvi@ispms.tsc.ru

Abstract. A new technology is developed for welding multi-span bridge constructions. The mechanical properties and structure of the low-carbon bridge steel welds have been studied. The welding parameters and application of steel-glass liners provide for long-term service of steel constructions in conformity with the welding industry specifications.

Introduction

Most critical steel constructions in Russia contain a multitude of non-detachable junction parts produced by the method of electric arc welding. This has led to a widespread use of field welding of all-climate bridge constructions, e.g. highway span bridges, foot bridges, including overpasses, viaducts, trestle bridges, etc. [see, e.g. STP 005-97 'Field welding technology of steel bridge constructions']. Field welding technologies are widely used in highway span bridge construction, which provides savings in materials, time and manpower. In particular, welding of roll stock having thickness up to 16 mm has been generally performed applying copper and glass-copper liners without cutting the wedges of the weld. Considering the extreme climatic conditions of the Far North and Siberia, fast heat removal from the copper liner frequently appears unwarranted. Since copper is expensive material, more cost-effective materials for welding liners are needed.

More specifically, new affordable liner material possessing low thermal conduction is required. This liner should provide a means for the preservation of the mechanical properties and uniform structure of the welded material in the area immediately adjacent to the weld. The researchers in [1] maintain that due to the insufficient heat removal from existing glass-copper liners, large-sized crystallites would form in the welding material at right angles to the welding pool, while small-sized crystallites aligned parallel to the glass-copper liner are much less numerous. Such structure is known to create imperfections in the welding junctions and often results in defects (cracks) in the butt joints of orthotropic plates near the longitudinal joints. These defects frequently occur during the longitudinal sliding of bridge spans in the process of bridge construction. For example, the longitudinal sliding of 30-m bridge spans along three-span pathway is known to cause crack initiation in 50% butt joints, although the stress level in the plates due to the longitudinal sliding did not exceed



150 MPa. The given paper is concerned with the glass-steel liner as an alternative material for the welding of bridge joints. The main purpose of the paper is to understand whether the glass-steel liner has better structural and mechanical properties allowing for less welding defects and cracks in the orthotropic bridge plates.

2. Research methods

The studies were performed for the samples of 12 mm thick model welds. The welds were produced by automatic welding on the horizontal plane of the low-carbon bridge steel (0.12-0.18% C, 0.4-0.7% Si, 0.4-0.7% Mn, 0.6-0.9% Cr, 0.3-0.6% Ni, 0.2-0.4% Cu, <0.035% P, <0.04% S, <0.08% As, <0.008% N) plates with glass-steel liners. There were also 8-mm gaps between the plates; no cutting of the weld edges was performed. First 50-mm long tack welds were manufactured at a distance of 200 mm from one another, using the E50 UONI-13/55 electrodes (GOST 9467-75). In so doing, manual adjustments were made between the welding operations. Next, the gap between the plates was filled with metal nibs prepared from the Sv-10NMA wire 2 mm in diameter. No chemical agents were used for initiating crystallization of the weld. Single pass welding was performed using the welding wire Sv-10NMA 3 mm in diameter; the flux AN-47 was also employed which had been subjected to calcination at 350-400°C. The welding station was equipped with a tractor ADF-1202 and a rectifier VDU-1202. The welding conditions were as follows: arc welding voltage and current 36 V and 800 A, respectively; welding productivity 18 m/h; electrode wire departure 12 mm.

The model weld sample had dimensions 500×400 mm²; its centerline weld joint was parallel to the long side of the sample. The following test samples were cut from the model weld samples in accordance with the GOST 6996–66.

a) The flat samples were tested by uniaxial static tension. These had dimensions 400×20×6 mm³; the weld was normal to the extension axis.

b) The samples subjected to free bend testing had a rectangular cross-section. The sample length was 170 mm; the sample had the same thickness as the plate, i.e. 12 mm; its width was equal to 1.5 plate thickness, i.e. 18 mm³. The weld was right in the middle of the sample; its bead was cut off.

c) The V-notch samples had the weld right in the middle and normal to the longitudinal axis. These were intended for impact testing in accordance with the GOST 9454–08.

The main mechanical properties of the welds were determined for the weld samples, which were tested in an Instron 1185 testing machine; the crosshead rate was 1 mm/min. The gauge length of the sample was 300 mm and the deformation rate was $5.5 \cdot 10^{-5} \text{ s}^{-1}$.

The samples were also tested in three-point slow bending in an Instron 1185 testing machine. The test fixture for three-point bends consisted of two cylindrical supports 25 mm in diameter. The separation between the supports was 110 mm, which determined the gauge length of the test sample. The test sample was arranged so that the weld root was at the bottom, i.e. in the area subjected to tension. The cylindrical bending mandrel was 25 mm in diameter; its rate was 5 mm/min. The test was stopped as soon as a crack appeared on the sample surface or the sample bended to 90°.

The value KCU⁻⁶⁰ was determined on an impact pendulum-type testing machine having maximum impact energy 300 J.

The macrostructure analysis of the cross-section of the weld metal was performed with the aid of deep etching method using nitrous-hydrofluoric acid solution in the 1:1 ratio. Metallographic sections were prepared from the weld metal and adjacent zones by polishing and etching in 4% alcohol solution of nitrous acid. The metallographic sections were used for examination of the microstructure of the weld material in the microscope 'Neophot-21'.

3. Discussion of Results

The microstructure of the weld material was examined using the metallographic cross-sections prepared from the samples tested by uniaxial static tension. The entire cross-section of the weld with the exception of the cap beads is presented in Fig. 1a. Evidently, the width of the weld zone exceeds

the thickness of the welded plates. A plausible explanation for this fact is too large volume of the welding bath coupled with too low rate of heat removal.

The weld had a coarse structure typical for most cast metals. The large dendrites were aligned horizontally with respect to the weld axis, which suggested that the heat removal had occurred mostly to the welded metal, which caused an insignificant growth of crystallites in the vicinity of glass liner (Fig. 1 a, b). Thus the macrostructure of the weld material had all the unfavorable features reported in [1]. Hence, the effectiveness of the technology in question must be assessed in terms of specifications of structural steels for bridge construction.

The main mechanical properties of the weld material were determined for the weld samples tested in tension [2]. The deformation curves were plotted for the test samples of as-received low-carbon bridge steel. These had a sharp yield point and a yield plateau. The physical yield strength, ultimate strength and plasticity were determined for the test samples; the values obtained were $\sigma_t = 368.9 \pm 6.8$ MPa; $\sigma_B = 537.3 \pm 2.9$ MPa and $\delta = 17.6 \pm 1\%$, respectively (cf. the values given in the GOST19282-73, i.e. $\sigma_{0.2} \geq 345$ MPa; $\sigma_B \geq 490$ MPa and $\delta \geq 21\%$ [3]). The latter value was probably due to the deformation behavior of the tensile sample. Thus the fracture probably occurred in the sample bulk, while the material of the weld and that of the adjacent zone remained practically non-deformed. The plasticity was determined for the entire test sample; hence a low value δ .

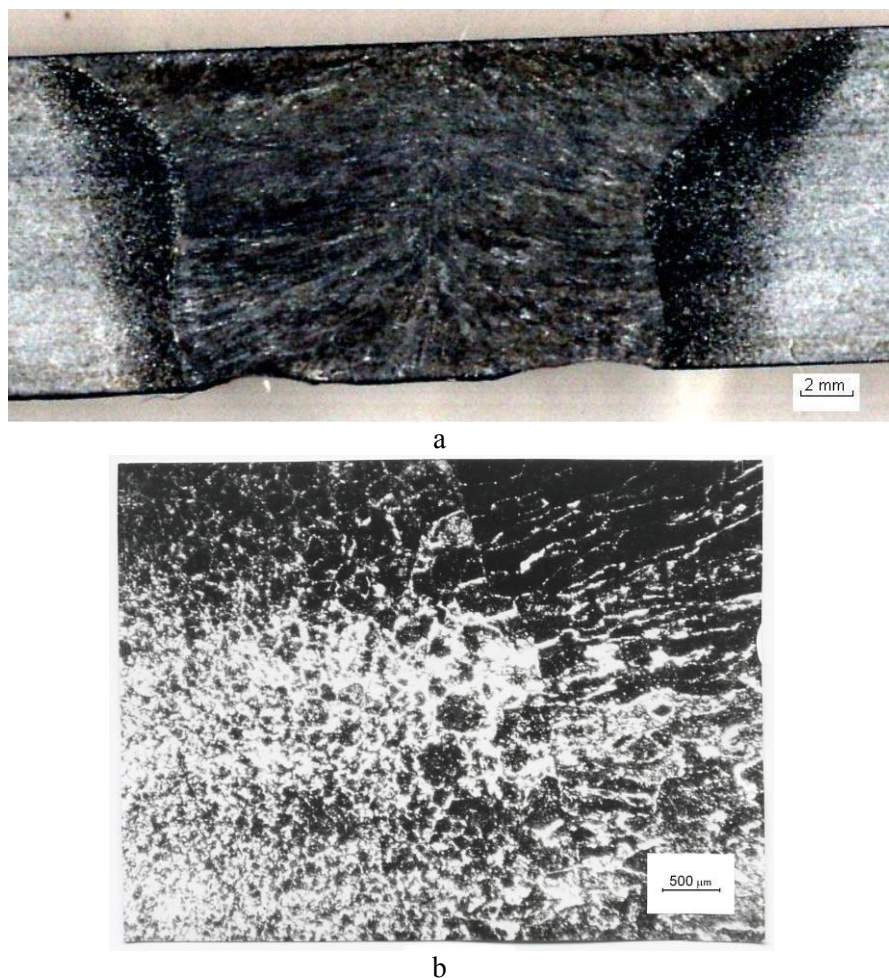


Figure 1. The macrostructure of the welding with glass-steel liner

The samples were tested in bending to an angle $\leq 90^\circ$. No cracks were observed for either the weld and heat-affected zone (HAZ) material or the bulk material. Therefore, all the samples were also tested in static bending.

The impact tests were carried on at the temperature -60°C . The resultant value $KCV^{-60} = 101.1 \pm 19.2 \text{ J/cm}^2$ was much higher than the value given in the GOST 19282–73 for the investigated steel, i.e. 34 J/cm^2 . All the test samples were found to undergo ductile-brittle fracture, with fibriform fracture surface showing large cleavage facets. The chemical composition of the V-notch zone of the weld differed from that of the base metal, since it had been altered due to the welding filler wire. The same zone had also greater thickness relative to that of the welded plates. Thus, the results of mechanical tests suggested that the weld joints with the glass-steel liner met all the requirements of the GOST specifications. It has been found that the macro-structure of the weld joints with glass liners is far from ideal. Evidently, the problem invites further investigation [4].

The base metal area immediately adjacent to the weld metal can be clearly seen in the macro-section; a portion of the macro-section is also illustrated in Fig. 1 (a, b, respectively). A well-defined difference apparently exists between the structure of the weld metal and that of the base metal on going from the fusion border to the original structure of the base metal (to the right and left sides of Fig. 1, respectively). The microstructure of the weld metal in zone I was examined (in what follows the zones are numbered in accordance with the classification in [4, 5]). The columnar crystals observed in the macro-section (Fig. 2) were defined as elongated ferrite plates with finely dispersed ferrite-cementite mixture occurring in between. In the course of material crystallization significant hydrogen-related stratification would probably occur.

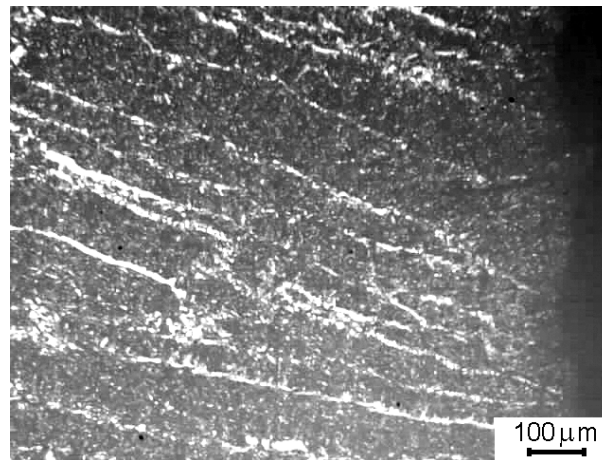
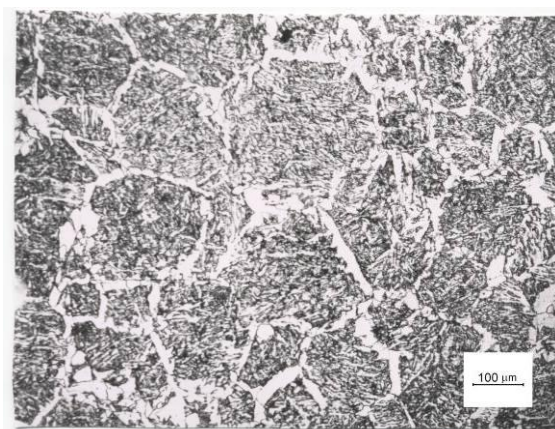
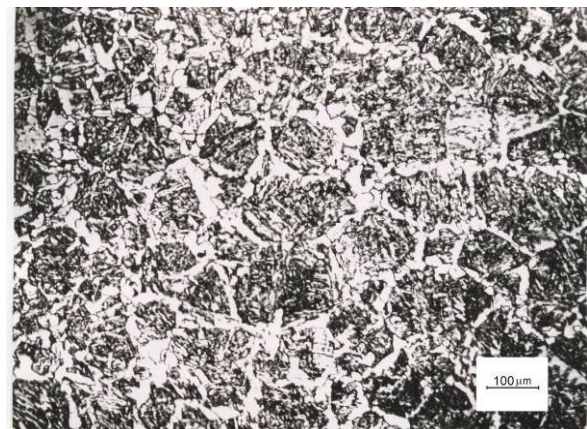


Figure 2. The microstructure of the weld metal in zone I



a



b

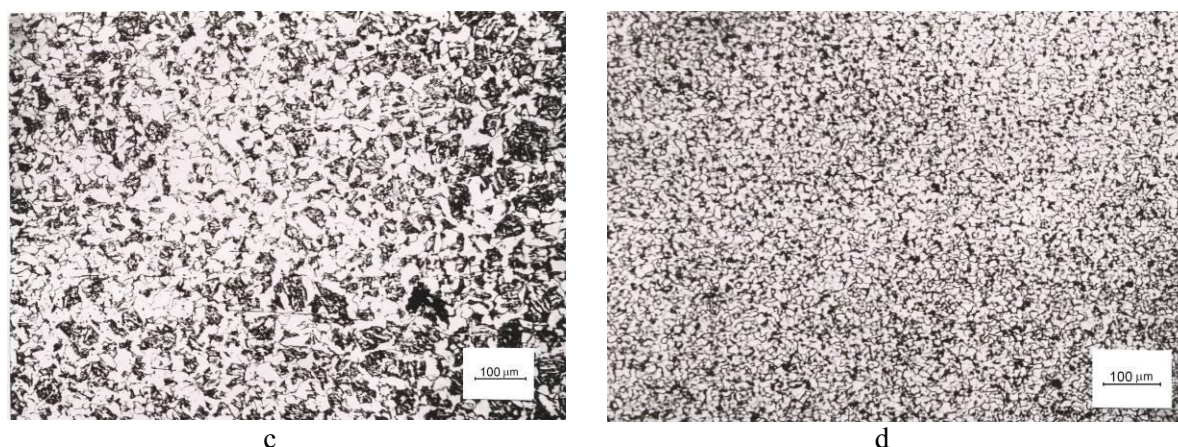


Figure 3. The microstructure of the weld material in zones V – VIII

The metal structure of the heat-affected zone 4.5 mm wide was distinguished by a dramatic inhomogeneity. Thus a narrow zone occurred in the vicinity of the fusion boundary where the temperature exceeded A_4 point (Fig. 1 a). The metal within this zone had an austenitic structure with medium-sized old austenitic grains elongated along the temperature gradient. This zone evidently corresponded to zones II, III and IV. The material of these zones has been subjected to a variety of thermal cycles, which was responsible for different types of discontinuities, e.g. transformation of austenite to δ -ferrite, local melting of austenite grain boundaries, formation of segregation areas and nonmetallic sulfide inclusions. The material of the melted zone would undergo crystallization, generally forming primary and secondary grain boundaries, depending on the cooling rate. In this case, ferrites were found to form at the primary austenitic grain boundaries and carbide particles, within the grains. The above transformations occurring within the HAZ might have had a drastic effect on the properties of the weld [4]. However, this investigation has provided no support for this view.

The material of the zone 1.25 mm in width has a coarse grain microstructure. According to the welding specification, the given area is a HAZ or zone V (Fig. 3 a) in which intensive austenite formation would occur. The microstructure of material of the latter zone was distinguished by the occurrence of Widmanstätten ferrite plates $\sim 20\ \mu\text{m}$ wide, which surrounded the primary austenitic grains having average size $\sim 300\ \mu\text{m}$, which contained misoriented thin ferrite plates. Besides, an insignificant amount of gas pores having size $20\ldots 30\ \mu\text{m}$ also occurred in the same zone.

Another zone is located on going from the fusion border down to a depth $\approx 1.9\ \text{mm}$ (Fig. 3 b). The material within the latter zone (VI) heated in the course of welding to the temperature exceeding A_3 point; however, the temperature was not sufficiently high to favor intensive growth of austenite. Thus the austenite formation also occurred in the base metal; however, the austenite grains had average size $\leq 150\ \mu\text{m}$. The austenite grains were also surrounded by Widmanstätten ferrite plates, which frequently broke at the grain boundaries, forming a set of polyhedral grains. The structure of the primary austenite grain was similar to that described above, although a more disperse one. Locally, diffusion transformation of the kind $\gamma \rightarrow \alpha$ took place with resultant formation of perlite eutectoids. The gas pores also occurred in the given zone; however, these were smaller than those of zone V.

4. Conclusion

The studies were carried on for the glass-steel liner welds. The mechanical properties of the welds from the low-carbon bridge steel were examined. The results suggest that the weld properties are in conformity with the GOST welding standards as well as the specifications of welding production. It has been found that the structure of the weld metal was far from perfect. Moreover, the width of the heat-affected zone was too large, which might cause problems by assembling and service of items. The structural defects might have emerged in the weld due to insufficient heat removal to the glass-steel liner, with the main energy flux passing through the base metal. To address the situation, the

energy flux might be reduced. In point of fact, the characteristic of the metal that is being welded and the joint type dictate the welding parameters. The methods for testing the weld material specified by the STP 005-97 are not sufficiently advanced to certify the weld joint. In particular, notch toughness is typically measured by the V-notch sample to provide information on the fracture toughness of the weld material. However, the experimental evidence obtained in this study suggests that the properties of the heat-affected zone are one of the significant factors to consider when evaluating the soundness of the weld joint.

Acknowledgement

The work was performed owing to the financial backing of the RFFI and in the frame of the RFFI grant N 14-08-00299; it was instrumentally supported by the 'Nanotech'.

References

- [1] V S Ageyev, S V Morozov, M P Shurygin, G I Nikonov, S A Shelkunov on the cause of crack initiation in the welds of orthotropic deck Transport Building 11 (2002) 18-20
- [2] E A Zernin, I R Sabirov, M A Kuznetsov The estimation of efficiency of welded joints Mining Informational and Analytical bulletin J Scientific and Technical Journal Issue 3 (2010) 318-322
- [3] V G Sorokin, V G Sorokin, M A Gevrashev Steels and Alloys Manual M Internet Engineering. (2001) 608
- [4] L S Livshits, A N Khakimov Physical metallurgy welding and thermal treatment of welds M Machine Building (1989) 336
- [5] D P Il'yaschenko, D A Chinakhov, V I Danilov, GV Shlyakhova, YM Gotovschik Increasing Strength and Operational Reliability of Fixed Joints of Tubes by MMA Welding IOP Conf Series Materials Science and Engineering **91** (2015)